Angular-ordered parton showers with medium-modified splitting functions

JHEP11(2009)122

(http://iopscience.iop.org/1126-6708/2009/11/122)

Published by IOP Publishing for SISSA

Received: *October 6, 2009*
Accepted: *November 13, 2009*
Published: *November 30, 2009*

Angular-ordered parton showers with medium-modified splitting functions

Néstor Armesto,[a] **Gennaro Corcella,**[b,c,d] **Leticia Cunqueiro**[e] **and Carlos A. Salgado**[a]

[a] *Departamento de Física de Partículas and IGFAE, Universidade de Santiago de Compostela, E-15706 Santiago de Compostela, Galicia, Spain*
[b] *Museo Storico della Fisica e Centro Studi e Ricerche E. Fermi, Piazza del Viminale 1, I-00184 Roma, Italy*
[c] *Scuola Normale Superiore, Piazza dei Cavalieri 7, I-56126, Pisa, Italy*
[d] *INFN, Sezione di Pisa, Largo Fibonacci 3, I-56127, Pisa, Italy*
[e] *INFN, Laboratori Nazionali di Frascati, Via E. Fermi 40, I-00044 Frascati, Roma, Italy*

E-mail: nestor.armesto@usc.es, gennaro.corcella@sns.it, lcunquei@cern.ch, carlos.salgado@usc.es

Abstract: Modified Altarelli-Parisi splitting functions were recently proposed to model multi-parton radiation in a dense medium and describe jet quenching, one of the most striking features of heavy-ion collisions. We implement medium-modified splitting functions in the HERWIG parton shower algorithm, which satisfies the angular ordering prescription, and present a few parton-level results, such as transverse momentum, angle and energy-fraction distributions, which exhibit remarkable medium-induced effects. We also comment on the comparison with respect to the results yielded by other implementations of medium-modified splitting functions in the framework of virtuality-ordered parton cascades.

Keywords: Hadronic Colliders, QCD, Jets

ArXiv ePrint: 0909.5118

doi:10.1088/1126-6708/2009/11/122

JHEP11(2009)122

Contents

JHEP11(2009)122

1 Introduction

Measurements performed at the Relativistic Heavy Ion Collider (RHIC) have emphasized the jet-quenching phenomenon, namely the suppression of particle production at large transverse momentum (p_T) with respect to the naive vacuum expectations, as well as other related phenomena, such as the disappearance or distortion of the particles directed in opposite azimuth to a triggered high-transverse-momentum one [1]. A typical explanation of jet quenching consists in assuming a higher radiative energy loss in a dense medium, which, with respect to the vacuum case, allows partons potentially produced at large p_T to further emit, in such a way to decrease the high-p_T multiplicity and enhance the low-p_T one. A lot of work has been undertaken in order to theoretically describe such effects [2]. Calculations carried out so far are suitable to predict inclusive quantities, but they are not adequate to describe exclusive final states, which is compelling for the experimental studies. Moreover, they deal with multi-parton emissions only by means of simple assumptions [3, 4].

As happens when studying hadron collisions in the vacuum, Monte Carlo event generators are the best possible tool for the sake of performing experimental analyses. In fact, Monte Carlo codes, such as the multi-purpose HERWIG [5] and PYTHIA [6] generators, contain fairly large libraries of hard-scattering processes, as well as initial- and final-state parton showers, models for hadronization and underlying event. Moreover, these programs provide one with exclusive final states: the user can set acceptance cuts on final-state particles and interface the Monte Carlo output with detector simulation programs. For such reasons, having Monte Carlo programs capable of simulating nucleus-nucleus interactions will be of great interest for the heavy-ion community working at RHIC [1] and ultimately at the LHC (see refs. [7–9] from ALICE, CMS and ATLAS experiments, respectively).

Although an algorithm for multiple radiation in a dense medium should require several a priori assumptions, it was recently proposed [10, 11] that a simple prescription to implement medium-induced effects in parton shower simulations consists in adding to the Altarelli-Parisi splitting function a term depending on the parameters which characterize

the medium, on the virtuality and on the energy of the branching parton. Under reasonable hypotheses on the medium properties, it was shown in [10] that, even allowing only one medium-modified splitting, it was possible to obtain azimuthal distributions qualitatively similar to the RHIC observations. Modified splitting functions have been recently implemented in the framework of the PYTHIA event generator [6]. This implementation is known under the name of Q-PYTHIA: the inclusion of modified splitting functions is detailed in [12], whereas the Q-PYTHIA fortran code can be downloaded from [13]. Although a thorough comparison with RHIC data has not yet been performed, the results of ref. [12] look in qualitative agreement with the expected features of heavy-ion collisions, namely suppression of particle production at large p_T, broader angular distributions and enhancement of intra-jet multiplicities.

In this paper we extend the method discussed in [10–12] and apply it to the HERWIG generator [5], the other general-purpose Monte Carlo program pretty much used by the experimental collaborations. In fact, having at least two codes implementing medium-modified splitting functions is mandatory for the sake of comparison and estimating the Monte Carlo uncertainty on a prediction. Also, it is well known that the algorithms implemented in HERWIG and PYTHIA are indeed quite different, in both parton showers and hadronization, which makes compelling including medium effects even in HERWIG and using it to analyse heavy-ion collisions.

In fact, HERWIG showers satisfy angular ordering of multiple soft radiation, which correctly accounts for colour coherence and allows one to probabilistically implement multiple soft emissions [14]. On the contrary, PYTHIA cascades are traditionally ordered according to the virtuality of the splitting parton, with an option to reject non-angular-ordered emissions. This was the scenario in which the authors of ref. [12] implemented modified splitting functions. The PYTHIA evolution variable is not, however, entirely equivalent to angular ordering in the soft limit: although in several cases the actual ordering variable does not make really big changes, when comparing with experimental observables sensitive to colour coherence, as done in ref. [15], HERWIG agrees with the data better than PYTHIA. Transverse-momentum ordering, included in the latest PYTHIA version [16], should yield a better description of angular ordering. Nevertheless, as discussed in [17], discrepancies with respect to HERWIG are still present when considering, e.g., the so-called non-global observables [18], sensitive to radiation in a limited part of phase space, such as the transverse energy flow in a rapidity gap. Even for the purpose of hadronization, the two programs implement very different models, namely the cluster model [19] (HERWIG), based on colour preconfinement, and the string model [20] (PYTHIA), both depending on a few parameters to be fitted to experimental data. It is only after turning hadronization on and fitting such models to the same data set (see, e.g. the study [21] for heavy-quark fragmentation) that the comparison between HERWIG and PYTHIA can be consistently made. At parton-level, due to the above mentioned differences in the treatment of parton showers, discrepancies between HERWIG and PYTHIA must instead be expected, in both vacuum and medium-modified cascades.

More generally, it is worthwhile pointing out that the choice of the ordering variable for multi-parton radiation in a medium is currently an open issue (see the discussion

JHEP11(2009)122

in [11]). For single-gluon emission, it is known that finite medium-size effects affect the radiation pattern by producing a suppression of small-angle emission, equivalent to the Landau-Pomeranchuk-Migdal effect [22]. Similar mechanisms may, for example, modify the suppression associated with colour coherence, which leads to angular ordering. Implementing medium-modified splitting functions in angular-ordered parton showers, as we shall do in this paper, or in virtuality-ordered cascades, as done in [12], will allow one to study how the jet structure in a medium depends on the adoption of a given evolution variable. Other approaches have also been pursued, following analytic or Monte Carlo methods [23]; the experience gained by applying all these different calculations and algorithms will be essential for a correct characterization of the underlying dynamics when experimental data from heavy-ion collisions will become available.

Hereafter, we shall employ the latest fortran version of HERWIG, with a few routines modified to include medium effects. The documentation of this code is currently in progress [24]: in the near future, the heavy-ion community will be able to compare the results of Q-PYTHIA with the ones of the medium-modified Q-HERWIG code. Furthermore, our work can be straightforwardly implemented even in the object-oriented C++ versions of HERWIG [25] and PYTHIA [26], containing the basic physics of the fortran ones, plus a number of remarkable improvements.

The plan of the present paper is the following. In section 2 we shall shortly review the basics of the HERWIG showering algorithm in the vacuum and how it differs with respect to the PYTHIA one. In section 3 we will discuss the implementation of the modified Altarelli-Parisi splitting functions and present results for the HERWIG Sudakov form factor. In section 4 we shall present a few parton-level results, showing the role played by medium effects. In section 5 we will summarize the main points of our investigation and make remarks on possible extensions of the analysis here presented.

2 The HERWIG parton shower algorithm

In this section we discuss the HERWIG algorithm in the vacuum, to which we shall apply later on the modifications due to a dense medium. Monte Carlo algorithms rely on the factorization of the branching probability for soft or collinear parton radiation. Referring to final-state radiation, the one mostly affected by medium effects, the probability of emission of a soft/collinear parton reads [14]:

$$d\mathcal{P} = \frac{\alpha_S}{2\pi}\frac{dQ^2}{Q^2}\; P(z)\; dz\; \frac{\Delta_S(Q^2_{\max}, Q^2_0)}{\Delta_S(Q^2, Q^2_0)}. \tag{2.1}$$

In (2.1), $P(z)$ is the Altarelli-Parisi splitting function, z the energy fraction of the radiated parton with respect to the emitter and Q^2 is the ordering variable of the shower, whose maximum and minimum values are $Q^2_{\max}$ and Q^2_0, respectively. $Q^2_{\max}$ is set by the hard-scattering process, whereas Q^2_0 is the user-defined scale at which the perturbative cascade ends and cluster hadronization starts [19].

In HERWIG [5] the evolution variable is $Q^2 = E^2\zeta$, where E is the splitting-parton energy and $\zeta = (p_1 \cdot p_2)/(E_1E_2)$, $p_1(E_1)$ and $p_2(E_2)$ being the momenta (energies) of the

JHEP11(2009)122

radiated partons. For massless partons, Q^2 turns out to be an energy-weighted angle, i.e. $Q^2 \simeq E^2(1-\cos\theta)$, where θ is the emission angle. For soft radiation, the HERWIG evolution variable is thus equivalent to angular ordering [14], valid in soft approximation, for azimuthally-averaged quantities, in the large-N_C limit. The scale of the strong coupling constant α_S is the transverse momentum of the radiated parton with respect to the emitter. In this way, one includes in the algorithm a class of subleading soft/collinear logarithms, thus improving the accuracy of the shower even beyond the leading-logarithmic approximation [27].

In (2.1) $\Delta_S(Q_1^2, Q_2^2)$ is the Sudakov form factor, expressing the probability of evolution from Q_1^2 to Q_2^2 with no resolvable emission; in diagrammatic terms, the Sudakov form factor sums up virtual and unresolved real emissions to all orders. The ratio of form factors in eq. (2.1) represents the probability that the emission at (z, Q^2) is the first, i.e. that there is no radiation during the evolution between $Q^2_{\max}$ and Q^2. It is given by the following expression:

$$\Delta_S(Q^2_{\max}, Q^2) = \exp\left\{ -\int_{Q^2}^{Q^2_{\max}} \frac{dk^2}{k^2} \int_{z_{\min}}^{z_{\max}} dz\ \frac{\alpha_S(z,k^2)}{2\pi}\ P(z) \right\}. \tag{2.2}$$

In eq. (2.2), the limits of the z-integration are given in HERWIG by[1] $z_{\min} = Q_0/Q$ and $z_{\max} = 1 - z_{\min}$.

The showering algorithm (2.1) is frame-dependent, however one can prove [14] that, if i and j are colour-connected partons, the upper values of the evolution variable satisfy the relation $Q_{i,\max} Q_{j,\max} = p_i \cdot p_j$, which is Lorentz-invariant. Hence, symmetric choices are made and $Q_{i,\max} = Q_{j,\max} = \sqrt{p_i \cdot p_j}$.[2] Furthermore, the energy of the parton which initiates the shower is fixed to $E_{\max} = Q_{\max}$: in this way, one identifies the HERWIG showering frame. Setting $Q^2 < Q^2_{\max}$ for the first emission yields $\zeta < 1$ ($\theta < \pi/2$ in the massless approximatiom) in the showering frame.

Although in the following we shall just deal with soft or collinear parton emissions, we point out that radiation of hard and large-angle partons can be implemented in HERWIG by applying matrix-element corrections. The region $\zeta > 1$, corresponding to hard and large-angle emissions, is the so-called 'dead zone' of the shower, where the exact amplitude is applied. Moreover, the 'hardest-so-far' emission in HERWIG showers is simulated according to the exact matrix element, thus allowing a smooth transition through the boundary of the dead zone [28].

Before discussing the implementation of medium effects, we wish to make a few comments on the difference between HERWIG and PYTHIA showering algorithms. As discussed in the introduction, PYTHIA includes colour coherence only partially: in [12], medium modifications were included in virtuality-ordered showers, with an option to reject emission which do not fulfil angular ordering. As for matrix-element corrections, PYTHIA

[1] As discussed in [12], the z-limits in PYTHIA, for a branching with virtuality p^2, are given by $z_{\min} = p_0^2/p^2$ and $z_{\max} = 1 - z_{\min}$, p_0^2 being the infrared cutoff. This yields on average a larger z-evolution range for PYTHIA.

[2] Such a choice implies, e.g., that for $e^+e^- \to q\bar{q}$ annihilation at energy $\sqrt{s}$, the initial value of the ordering variable for q and $\bar{q}$ is $Q_{\max} = \sqrt{s/2}$.

JHEP11(2009)122

has no dead zones: it uses the soft/collinear approximation throughout all physical phase space and simulates only the first branching via the exact amplitude [29]. Hadronization is finally implemented in PYTHIA following the string model [20]. Since parton showers and possible matrix-element matching are implemented in a pretty different way, if one studies parton-level quantities, as will be done hereafter, HERWIG results should not necessarily agree with the PYTHIA ones presented in [12], even though one models medium effects in the same way.

Of course, we are aware that a comparison of the results yielded by HERWIG and PYTHIA is compulsory. However, it can be meaningfully done only at hadron-level and after both generators are tuned to the same data. In this work, we shall restrict ourselves to comment on possible discrepancies at parton level and leave to future work a more detailed comparison, which will demand the redoing of the previous extensive studies in hadron-hadron collisions.

3 Medium-modified splitting functions

In this section we discuss the main issues concerning the implementation of medium effects in parton shower algorithms. We follow the method presented in [10, 11] and add to the Altarelli-Parisi splitting function in the vacuum $P(z)$ a medium-dependent term $\Delta P(z, p^2, E, \hat{q}, L)$:

$$P(z) \to P(z) + \Delta P(z, p^2, E, \hat{q}, L). \tag{3.1}$$

In (3.1), p^2 is the branching-parton virtuality, E its energy, L the medium length, $\hat{q}$ the transport coefficient, defined as the average transverse momentum transferred from the medium to the parton per unity of free path [3]. Hereafter, we shall often make use of the quantities $\hat{q}L$, the so-called accumulated transverse momentum, and of the frequency $\omega_c = \hat{q}L^2/2$.

The transformation (3.1) will be applied to the branching algorithm (2.1) and, in particular, to the integrand function of the Sudakov form factor (2.2), taking care that HERWIG evolution variable is not the virtuality p^2, but the energy-weighted angle Q^2 defined above.[3] As in [12], a crucial hypothesis on which our work is based is that, even in a dense medium, the factorization (2.1) between branching and no-branching probability still holds and that the showering evolution variable is the same as in the vacuum. In HERWIG, this means that we shall assume angular ordering and colour coherence even for parton cascades in a medium. In other words, the colour flow will not be modified with respect to its vacuum pattern.

Following [11], we shall modify the splitting functions for the branchings $q \to qg$ and $g \to gg$, while we shall assume that the splitting $g \to q\bar{q}$ gets negligible medium modifications.[4] $\Delta P(z, p^2, E, \hat{q}, L)$ can be expressed in terms of the medium-induced parton

[3] For soft/collinear radiation, it is straightforward to show that the relation $p^2 \simeq 2z(1-z)Q^2$ holds.

[4] In any case, the splitting $g \to q\bar{q}$ is quite uncommon in the shower, since the splitting function $P_{qg}(z) = T_R[z^2 + (1-z)^2]$ is not soft-enhanced. It is only after turning cluster hadronization on [19] that non-perturbative $g \to q\bar{q}$ splittings are forced and $P_{qg}(z)$ plays a role.

JHEP11(2009)122

radiation spectrum $I^{\rm med}(z,p^2)$, computed in the so-called BDMPS approximation [30–32]:

$$\Delta P(z,p^2,E,\hat{q},L) \simeq \frac{2\pi p^2}{\alpha_S}\frac{d^2 I^{\rm med}}{dz dp^2}. \tag{3.2}$$

As discussed in [12], eq. (3.2) gives the medium corrections to the soft-divergent part of the Altarelli-Parisi splitting functions; the finite terms are assumed to be vacuum-like.[5]

$\Delta P(z,p^2,E,\hat{q},L)$ can be expressed in terms of the energy E of the parent parton and of the dimensionless variables E/ω_c and $\kappa^2 = k_T^2/(\hat{q}L)$, where k_T is the transverse momentum of the radiated soft/collinear parton with respect to the splitting one. For multiple radiation, E will always be the energy of the splitting quark/gluon. As for the medium length, if L_0 is the length for the first splitting, for the following emissions we have to take into account that a radiated parton, with energy fraction z, travels for a distance $2zE/k_T^2$, the so-called parton formation length, before splitting again. Therefore, the effective medium length for subsequent branchings will be:

$$L = L_0 - \frac{2zE}{k_T^2}. \tag{3.3}$$

We note that in eq. (3.3) L is not positive definite and, especially for small values of L_0 and very soft/collinear splittings, it may well become negative after few emissions. Whenever this is the case, we shall assume that the shower continues in a vacuum-like fashion.

In ref. [11] the modified Altarelli-Parisi splitting functions were implemented in a Sudakov form factor computed in the same way as PYTHIA does. It was indeed found that medium effects have a remarkable impact and, for any given values of $\hat{q}$ and L, the Sudakov form factor is suppressed with respect to the vacuum one in the full p^2-range, for both quarks and gluons. As a decreasing of the form factor corresponds to an enhancement of the branching probability, a higher parton multiplicity in the medium-modified shower must be expected. This was indeed found in [12] using Q-PYTHIA: although for a consistent comparison with data one must turn hadronization on, such an observation is in qualitative agreement with the expectations from radiative energy loss [1].

In figure 1 we present the HERWIG Sudakov form factor, possibly including medium effects by means of eq. (3.1); for simplicity, we plot $\Delta(Q^2, Q^2_{\rm max})$ with fixed E and $L = L_0$, as if we were dealing with the the first emission in the shower. We consider medium-induced showers initiated by gluons of energy $E = 10$ and $100\,\text{GeV}$ and media with $\hat{q} = 1$ and $10\,\text{GeV}^2/\text{fm}$, $L_0 = 2$ and $5\,\text{fm}$. In the following, for the sake of brevity, we shall label such medium configurations in terms of the accumulated transverse momentum, say $\hat{q}L_0 = 2$, 5, 20 and $50\,\text{GeV}^2$; the corresponding values of $\hat{q}$ and L_0 are left understood. For gluon-initiated showers, the lower value of the evolution variable is, by default, $Q_0 \simeq 1.7\,\text{GeV}$ [5], whereas we set by hand the upper value[6] $Q_{\rm max} = \sqrt{2}\,E$. From figure 1 we learn that

[5] That means that, e.g., for a $q \to qg$ branching, where the Altarelli-Parisi splitting function is given by $P_{gq}(z) = C_F[1+(1-z)^2]/z$, medium-induced modifications affect the overall $\sim 1/z$ factor, while the finite-z corrections remain unchanged.

[6] The maximum value for the virtuality-ordered PYTHIA showers used in [12] is $p^2_{\rm max} = 4E^2$. Hence, even the p^2-evolution range in PYTHIA is larger than the Q^2 one in HERWIG.

JHEP11(2009)122

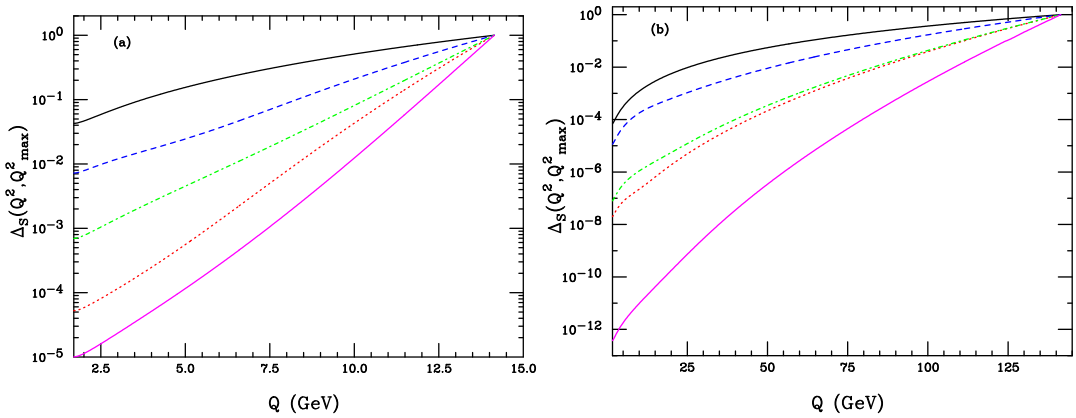

Figure 1. Gluon Sudakov form factors, in the vacuum (solid, black) and in media with $\hat{q}L_0 = 2$ (dashes, blue), 5 (dots, red), 20 (dot-dashes, green) and 50 (magenta, solid) GeV^2. The shown cases correspond to starting energies of $E = 10\,\text{GeV}$ (a) and 100 GeV (b). (For the interpretation of the references to colours in all figure legends, the reader is referred to the online version of this paper).

medium-induced effects are pretty relevant: for both E=10 and 100 GeV, the suppression due to including $\Delta P(z, p^2, E, \hat{q}, L)$ can be up to several orders of magnitude, especially for relatively small values of Q. Of course, when Q approaches Q_{max}, all form factors tend to 1, and therefore the discrepancy due to the different values of $\hat{q}L_0$ tends to become smaller, but it is nonetheless well visible throughout all Q-range. As for the behaviour of the modified $\Delta_S(Q^2, Q^2_{\text{max}})$ when $\hat{q}$ and L_0 change, we find that, for both E values and in all Q-range, the highest no-branching probability is obtained for $\hat{q}L_0 = 2\,\text{GeV}^2$ and the lowest for $\hat{q}L_0 = 50\,\text{GeV}^2$, as one should indeed expect. The comparison between the other two options in instead more cumbersome: for $E = 10\,\text{GeV}$, $\Delta_S(Q^2, Q_{\text{max}})$ for $\hat{q}L_0 = 20\,\text{GeV}^2$ is much larger than the form factor for $\hat{q}L_0 = 5\,\text{GeV}^2$, thus implying more branching in the case of accumulated transverse momentum equal to $5\,\text{GeV}^2$. For $E = 100\,\text{GeV}$, the $\hat{q}L_0 = 20\,\text{GeV}^2$ form factor is above the $\hat{q}L_0 = 5\,\text{GeV}^2$ one at low Q, but for Q values larger than 70-80 GeV, which roughly correspond to the first branchings in the shower, they are very close to each other.[7] Therefore, we can already foresee some similarities between these two medium parametrizations in the phenomenological analysis which we shall carry out for $E = 100\,\text{GeV}$. In any case, the splitting-parton energy and the medium length vary throughout the cascade and figure 1 has been instead obtained for fixed L_0 and E; the plotted $\Delta_S(Q^2, Q^2_{\text{max}})$, though very useful to give us a qualitative estimate of the medium suppression, are not exactly the ones which we shall implement within the HERWIG algorithm.

Since the ordering variables in PYTHIA and HERWIG are different, the numerical comparison between figure 1 and the Sudakov form factors presented in [11] is not straightforward. However, as we said before, since the evolution range for variables z and Q^2 in

[7] Note that the radiative energy loss is not only function of the product $\hat{q}L_0$, but its dependence on $\hat{q}$ and L_0 is more complex.

JHEP11(2009)122

HERWIG is narrower than for the corresponding PYTHIA quantities, at least in the default scenarios, we can already predict a stronger medium-induced Sudakov suppression and more branchings in PYTHIA rather than in HERWIG, in both vacuum and medium-modified showers.

4 Results

In this section we will present some phenomenological results showing the impact of medium modifications in HERWIG. In [12], as a case study, the authors considered a gluon with fixed energy, giving rise to a medium-modified cascade within the PYTHIA model. This is not a standard option in HERWIG, but nevertheless, for the sake of comparison, we implemented a fictitious process with a single gluon of given energy E initiating a shower. In PYTHIA virtuality evolution, this was relatively straightforward, whereas in HERWIG, since one has angular ordering, in principle one would need two colour-connected partons to define the initial value of the evolution variable $Q^2_{\max}$. Still, we managed to start with a gluon of energy E, setting by hand the upper value of the evolution variable $Q^2_{\max} = 2E^2$. Subsequent splittings ($g \to gg$ and so forth) will follow standard colour coherence.[8] Similar tricks would be necessary if one wanted to simulate such a fictitious process in PYTHIA, but with showers ordered in transverse momentum, as their implementation follows a dipole formalism and one would need to start with two colour-connected partons [16]. Furthermore, as we are not investigating an actual physical process, we turn matrix-element corrections off; how to implement exact higher-order corrections to the hard-scattering process in a medium is anyway an open issue.

As in [12], we shall study the distributions of the transverse momentum p_T of final-state partons, the emission angle θ, with respect to the initial-gluon axis, and the logarithmic energy fraction, defined as $\xi = \ln(E/|p|)$, $|p|$ being the modulus of the parton momentum. As we said before, we consider showers in the vacuum and in a dense medium characterized by parameters $\hat{q}$ and L_0. We shall assume gluon energies $E = 10$ and $100\,\mathrm{GeV}$ and, as in the previous section, medium parameters leading to $\hat{q}L_0 = 2$, 5, 20 and $50\,\mathrm{GeV}^2$. Throughout the cascade, the effective medium length L will be obtained by applying eq. (3.3); our distributions will be labelled in terms of the accumulated transverse momentum $\hat{q}L_0$.

Though being an unphysical quantity, it is interesting to compute first the average parton multiplicity $\langle N \rangle$ in the vacuum and in media characterized by the parameters given above. Such multiplicities strongly depend on the shower cutoff Q_0 and obviously increase whenever Q_0 is lowered. In table 1 we quote these numbers for default HERWIG and different values of $\hat{q}L_0$: as expected, parton multiplicities increase in a dense medium, which is in agreement with the measurements of larger medium-induced energy loss. For $E = 10\,\mathrm{GeV}$, the enhancement runs from 20% ($\hat{q}L_0 = 2\,\mathrm{GeV}^2$) up to about 80% ($\hat{q}L_0 = 50\,\mathrm{GeV}^2$); for $E = 100\,\mathrm{GeV}$ the corresponding numbers are 7% and 70%. It is interesting to notice in table 1 that the cases $\hat{q}L_0 = 5$ and $20\,\mathrm{GeV}^2$ give quite similar results and that the $\hat{q}L_0 = 20\,\mathrm{GeV}^2$ multiplicity is slightly above the $\hat{q}L_0 = 5\,\mathrm{GeV}^2$ one for $E = 10\,\mathrm{GeV}$

[8] As an alternative option, one can run the fictitious process $e^+e^- \to gg$ at $\sqrt{s} = 2E$, available in the HERWIG library, and study the parton shower only in one hemisphere.

JHEP11(2009)122

E	$\hat{q}L_0 = 0$	$\hat{q}L_0 = 2\,\mathrm{GeV}^2$	$\hat{q}L_0 = 5\,\mathrm{GeV}^2$	$\hat{q}L_0 = 20\,\mathrm{GeV}^2$	$\hat{q}L_0 = 50\,\mathrm{GeV}^2$
10 GeV	2.56	3.05	4.14	3.60	4.56
100 GeV	6.95	7.41	8.79	8.93	11.70

Table 1. Average parton multiplicities in HERWIG showers initiated by gluons of energy of 10 and 100 GeV, in the vacuum and in a medium with assigned values of $\hat{q}L_0$.

and below for a gluon of 100 GeV. In fact, the modified splitting functions (3.2) do not scale with respect to $\hat{q}L_0$ and do depend on the initiating parton energy: therefore, the phenomenological implications of the introduction of medium effects depend on the three variables $\hat{q}$, L_0 and E and different behaviours are to be expected if we start the cascade with partons of different energies, even though we use same values of $\hat{q}$ and L_0. In figure (1), although the Sudakov form factors were computed for fixed E and L, we already noticed differences between the options $\hat{q}L_0 = 5\,\mathrm{GeV}^2$ and $\hat{q}L_0 = 20\,\mathrm{GeV}^2$, according to whether we have $E = 10$ or 100 GeV. In figures 2–4 we present the p_T, θ and ξ distributions, according to HERWIG in the vacuum and in a medium with the parameters $\hat{q}$ and L_0 stated before, for energies $E = 10$ GeV (a) and 100 GeV (b). We plot everywhere normalized parton multiplicities, such as $(1/N)\ dN/dp_T$, so that the total integral will be equal to 1.[9] A feature of the vacuum spectra at 10 GeV is that they exhibit a sharp peak at $p_T = \xi = \theta = 0$, corresponding to events where the initiating gluon evolves down to the shower cutoff with no branching at all. The probability for this to happen depends on the Sudakov form factor $\Delta_S(Q^2_{\mathrm{max}}, Q^2_0)$, hence it may be eventually lowered by decreasing Q_0 or increasing Q_{max}, thus allowing more radiation in the evolution. Also, such a spike will vanish once hadronization is turned on. A peak, though less sharp, is visible even for media with small values of $\hat{q}L_0$, e.g. $\hat{q}L_0 = 2\,\mathrm{GeV}^2$, whereas it disappears for larger values of $\hat{q}L_0$. Also, it is less visible for $E = 100$ QeV, as in this case $Q_{\mathrm{max}} \simeq 141.42$ GeV and $\Delta(Q^2_{\mathrm{max}}, Q^2_0)$ is a pretty small non-emission probability.[10] It is interesting to notice that, even for $E = 10$ GeV, such a peak was not so visible in [12], where the authors did find some events with no radiation, but, since the branching probability in the PYTHIA model is higher that in HERWIG in all evolution range, the Q-PYTHIA spectra exhibit smooth behaviour, even when p_T, θ or ξ approach zero. Later in this section, as an example, we shall plot integrated parton multiplicities, which behave smoothly also in the very first bin of our histograms. As for the p_T spectra, i.e. figure 2, for E=10 GeV the vacuum distribution is above the others at large p_T, as in [12]; however, due to the presence of the $p_T = 0$ peak, such a behaviour is less evident than in PYTHIA. In both cases, it is anyway the $\hat{q}L_0 = 5\,\mathrm{GeV}^2$ curve the one that gives the lowest normalized multiplicity at large p_T. At low p_T, Q-PYTHIA gives the highest parton multiplicity in the two scenarios corresponding to $L = 5$ fm; the lowest multiplicity was instead the one for the vacuum

[9] On the contrary, the plots presented in ref. [12] are normalized to the mean parton multiplicity; rescaling our distributions to the multiplicities in table 1 is straightforward.

[10] A similar effect was found, e.g., in ref. [33], where the simulation of W/Z transverse momentum at the Tevatron exhibited a sharp peak at $p_T = 0$, which disappears whenever one sets a non-zero intrinsic transverse momentum for the incoming partons.

JHEP11(2009)122

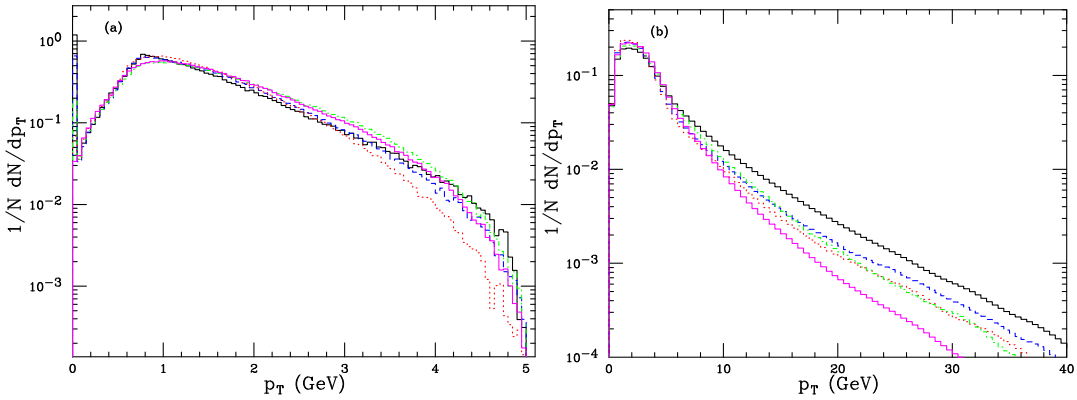

Figure 2. Transverse momentum multiplicity for a medium-modified shower initiated by a gluon of energy 10 GeV (a) and 100 GeV (b), in the vacuum (solid, black) and in media with accumulated transverse momentum $\hat{q}L_0 = 2$ (dashes, blue), 5 (dots, red), 20 (dot-dashes, green) and 50 (solid, magenta) GeV^2.

case [12]. In HERWIG the low-p_T distribution is clearly affected by the $p_T \to 0$ behaviour: the spectra exhibit a maximum about $p_T = 1$ GeV, but, up to $p_T \simeq 0.8$ GeV, the difference between the four chosen $\hat{q}L_0$ is quite small. For $E = 100$ GeV, the absence of a significant event fraction with no showering makes it easier to compare with the results yielded by Q-PYTHIA. Overall, for the reasons discussed above, namely lower effects in the Sudakov form factor, the impact of the implementation of medium modifications in HERWIG looks smaller than in Q-PYTHIA. However, the behaviour with respect to varying $\hat{q}$ and L_0 is qualitatively the same. The vacuum spectrum is the lowest at small p_T and the highest at large p_T, where the $\hat{q}L_0 = 50$ GeV^2 distribution is the one going to zero more rapidly. The other three curves, corresponding to $\hat{q}L_0$=2, 5 and 20 GeV^2, lie in the range of the two extreme cases, as one should expect. In particular, at large p_T, $\hat{q}L_0 = 5$ and 20 GeV^2 seem to give similar distributions, whereas the $\hat{q}L_0 = 2$ GeV^2 option yields the largest high-p_T normalized multiplicity after the vacuum.

Concerning the θ spectra, i.e. figure 3, first of all we need to point out an essential difference between HERWIG and PYTHIA angular distributions, independently of medium effects. PYTHIA, which does not systematically implement angular ordering, allows parton radiation in all allowed phase space, i.e. up to $\theta = \pi$; on the contrary, in HERWIG angular-ordered showers, radiation is possible only for $\zeta < 1$, ζ being the showering variable defined in section 2. This leads to an empty region in the physical phase space, corresponding to large-angle emission. More precisely, in the massless approximation, the condition $\zeta < 1$ implies $\theta < \pi/2$ in the HERWIG showering frame. At the end of the showering, however, when jets acquire mass, a Lorentz boost is applied: this enlarges the angular permitted region, but a zone where radiation is forbidden is still present. In a physical process, such as $e^+e^- \to q\bar{q}$, this empty region would be filled by the soft radiation from the other jet, i.e. from $\bar{q}$ if one triggers the shower initiated by q.[11] However, as we are simulating an unphysical process with only a single coloured parton, a dead zone, corresponding to

[11] In any case, even with two jets, there will still be a missing region, due to hard and wide-angle radiation, that one should eventually fill by means of matrix-element corrections.

JHEP11(2009)122

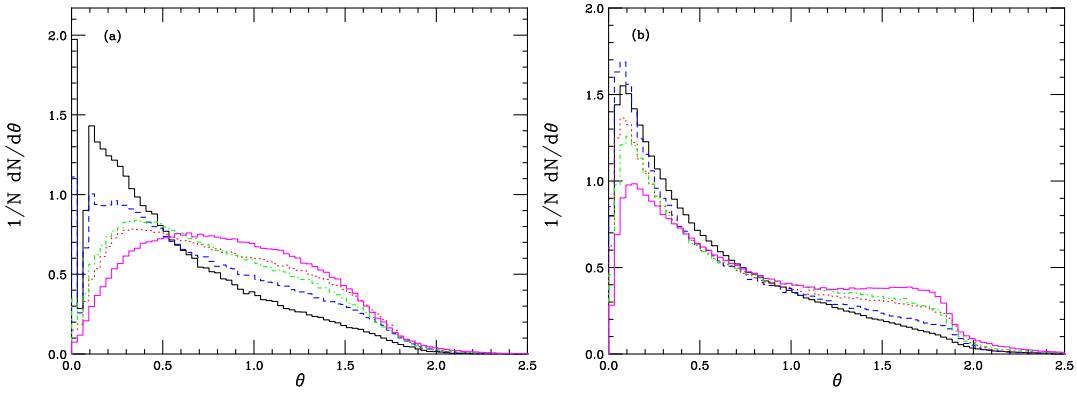

Figure 3. As in figure 2, but showing the angular distributions for showers initiated by a gluon of energy 10 GeV (a) and 100 GeV (b), in the vacuum and in a dense medium.

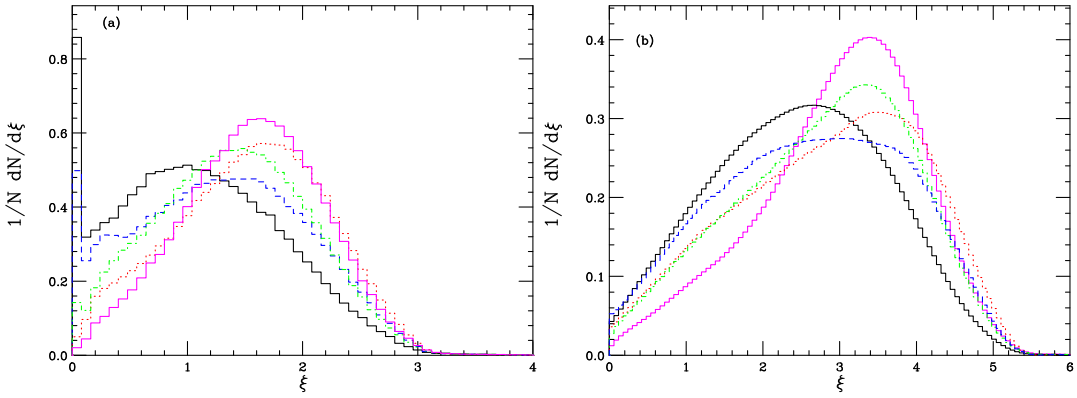

Figure 4. As in figures 2 and 3, but presenting the logarithmic energy-fraction (ξ).

large-angle radiation off the primary gluon, must be expected.

In fact, the spectra in figure 3 show that the parton multiplicity above $\theta \simeq 2$ is negligible. As medium modifications mostly affect the first few emissions, which, because of angular ordering, are the ones at the largest θ, it is reasonable that the spectra in a dense medium are above the vacuum ones in $1 < \theta < 2$, as we learn from figure 3. At small θ, i.e. far from the hard scattering, the parton formation length $2zE/k_T^2$ is likely to be large and the effective medium length L, given by eq. (3.3), becomes negative. This implies that small-angle branchings are typically vacuum-like. As far as the different $\hat{q}L_0$ options are concerned, the $\hat{q}L_0 = 2\,\mathrm{GeV}^2$ is clearly the closest to the vacuum prediction, the difference between $\hat{q}L_0 = 5$ and $20\,\mathrm{GeV}^2$ is small, though visible, whereas the $\hat{q}L_0 = 50\,\mathrm{GeV}^2$ spectrum, corresponding to the strongest medium modifications, leads to the highest parton multiplicity in the allowed large-angle range, say $1 < \theta < 1.8$. We finally comment on the logarithmic energy-fraction (ξ) plots, presented in figure 4. As for the $E = 10\,\mathrm{GeV}$ case, the $\xi = 0$ peak clearly spoils the low-ξ part of the spectrum. However, regardless of such a peak, the suppression of partons with small energy fraction in a dense medium with respect to the vacuum is still clear. The behaviour of the four medium-

JHEP11(2009)122

modified spectra in terms of $\hat{q}$ and L_0 is alike the one displayed in [12]. At small ξ, the $\hat{q}L_0 = 2\,\mathrm{GeV}^2$ spectrum yields the highest energy fraction, followed, in order, by $\hat{q}L_0 = 20$, 5 and $50\,\mathrm{GeV}^2$. Around the peak, the order is reversed, with $\hat{q}L_0 = 50\,\mathrm{GeV}^2$ giving the largest event fraction and $\hat{q}L_0 = 2\,\mathrm{GeV}^2$ the lowest. At large ξ, the difference due to the different options of $\hat{q}L_0$ tends to become smaller; at very high ξ, the $\hat{q}L_0$=5 GeV^2 spectrum is above the others. For $E = 100\,\mathrm{GeV}$, since the events without emissions are very few, the comparison among the different curves and the results in [12] is straightforward. The low-ξ suppression in a medium with respect to the vacuum is still remarkable: within the modified spectra, at small ξ, the $\hat{q}L_0 = 2\,\mathrm{GeV}^2$ option yields the highest event fraction, followed by $\hat{q}L_0 = 5$ and $20\,\mathrm{GeV}^2$, whose results are roughly similar, and finally $\hat{q}L_0 = 50\,\mathrm{GeV}^2$. At large ξ, the order of the different $\hat{q}L_0$ cases is reversed, as happens for E=10 GeV.

The presence of a peak for a gluon with $E = 10\,\mathrm{GeV}$, whenever p_T, ξ or θ are close to zero, can be a bit disturbing, since we have a non-negligible fraction of events in the very first histogram bin, affecting overall the full spectrum. As we said, a possibility to reduce the events in the first bin consists in enlarging the evolution range or turning hadronization on. As an alternative, for the time being, we can compute integrated quantities, such as, e.g., parton multiplicities up to a given value of ξ, namely:

$$N(\xi) = \int_0^{\xi} d\xi' \frac{dN}{d\xi'}. \tag{4.1}$$

In figure 5 we plot $N(\xi)$ in the vacuum, for the four chosen scenarios of $\hat{q}$ and L_0, and $E = 10\,\mathrm{GeV}$: we observe a well visible medium-induced suppression at small ξ with respect to the vacuum. At low energy fractions, e.g. $\xi \simeq 0.5$, we find that the medium suppression is about 10% for $\hat{q}L_0 = 2\,\mathrm{GeV}^2$ and can be up to 60% for accumulated transverse momentum $\hat{q}L_0 = 50\,\mathrm{GeV}^2$. As we said in the introduction, although an actual comparison would require hadronization corrections and possible tuning of the Monte Carlo parameters to the data, such results are indeed quite encouraging, as they are in qualitative agreement with the small-ξ suppression observed at RHIC.

Before closing this section, following [12], we wish to study the p_T, θ and ξ distributions for fixed values of the medium length throughout the parton cascade. This means that, instead of applying eq. (3.3) at each branching, we shall always employ $L = L_0$. In fact, because of eq. (3.3), the medium length could even become negative at some point, which implies that, after the first few branchings, emissions occur in a vacuum-like fashion. For $L = L_0$, therefore, the medium length will always stay positive, and stronger medium effects are to be expected. As a case study, we investigate the two options $\hat{q}L_0 = 2$ and $\hat{q}L_0 = 50\,\mathrm{GeV}^2$, for variable and fixed medium length, and still $E = 10$ and 100 GeV. We first calculate the average parton multiplicity $\langle N \rangle$: we obtain, for $L = L_0$ and $E = 10\,\mathrm{GeV}$, $\langle N \rangle \simeq 3.17$ and 4.92, for $\hat{q}L_0 = 2$ and $50\,\mathrm{GeV}^2$, respectively. This corresponds to enhancements of 4% and 8% with respect to the variable-length results in table 1. For an initiating gluon of energy 100 GeV, the average multiplicities are $\langle N \rangle \simeq 8.09$ ($\hat{q}L_0 = 2\,\mathrm{GeV}^2$) and $\langle N \rangle \simeq 19.23$ ($\hat{q}L_0 = 50\,\mathrm{GeV}^2$), hence the enhancement runs from 10% to 65%. Such results are in agreement with the expectation that a fixed length should emphasize medium-induced effects.

JHEP11(2009)122

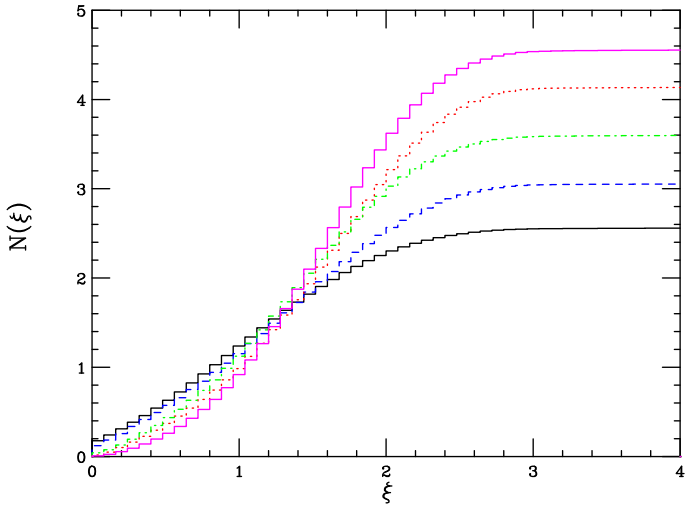

Figure 5. Integrated ξ distribution in the vacuum (solid, black) and in a medium with $\hat{q}L_0 = 2$ (dashes, blue), 5 (dots, red), 20 (dot-dashes, green) and 50 (solid, magenta) GeV^2. The energy of the gluon initiating the parton shower has been set to 10 GeV.

A more evident impact of medium modifications is also exhibited by the p_T, θ and ξ normalized spectra, presented in figures 6–8. In fact, for $L = L_0$, the suppression at large p_T and the enhancement at small p_T, displayed by figure 6, is stronger than what found when varying L according to eq. (3.3). The effect is milder for $\hat{q}L_0 = 2\,\text{GeV}^2$, as we are starting from small medium parameters, whereas it gets quite remarkable for $\hat{q}L_0 = 50\,\text{GeV}^2$ and $E = 100\,\text{GeV}$. In the angular distributions (figure 7), for $\hat{q}L_0 = 2\,\text{GeV}^2$ the effect of fixing L is small but visible, while, for $\hat{q}L = 50\,\text{GeV}^2$, the fixed-length angular spectrum is above the variable-L one for $0.4 < \theta < 1.2$ and below at larger angles. In fact, setting $L = L_0$, quarks and gluons always 'see' a positive medium length, and partons, which in the variable-L cascade would be potentially produced at large θ, are now allowed to further branch. This explains why, for fixed L, we have a smaller *normalized* multiplicity at very large angles and a higher one at middle θ-values. As all distributions are normalized to unity, the fixed-L spectrum is above the variable-L one at small angles. Stronger suppression (enhancement) at small (large) values of ξ is also exhibited by the energy-fraction plots in figure 8, especially for $\hat{q}L_0 = 50\,\text{GeV}^2$.

5 Conclusions

We implemented medium-modified splitting functions in the HERWIG parton shower algorithm, whose evolution satisfies the angular ordering prescription. Following the Q-PYTHIA implementation detailed in [12], we added to the Altarelli-Parisi splitting function a term depending on the medium properties, the virtuality and the energy of the radiating parton. Such a modification was consistently implemented in both branching probability and Sudakov form factor.

JHEP11(2009)122

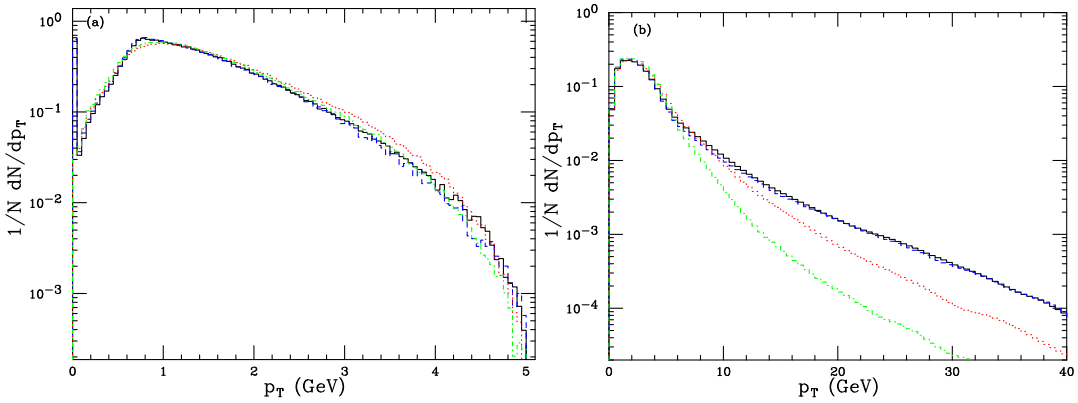

Figure 6. Transverse momentum distribution, with variable and fixed medium length L. The considered cases are $\hat{q}L_0 = 2\,\mathrm{GeV}^2$ (black, solid: variable L; dashes, blue: fixed L) and $\hat{q}L_0 = 50\,\mathrm{GeV}^2$ (red, dots: variable L; green, dot-dashes: fixed L), with an initiating gluon of 10 GeV (a) and 100 GeV (b).

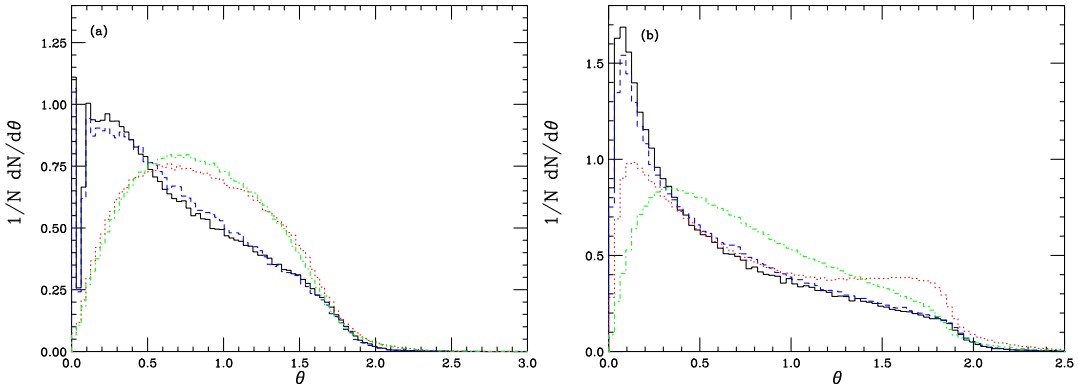

Figure 7. As in figure 6, but displaying the angular distributions for variable and fixed medium length.

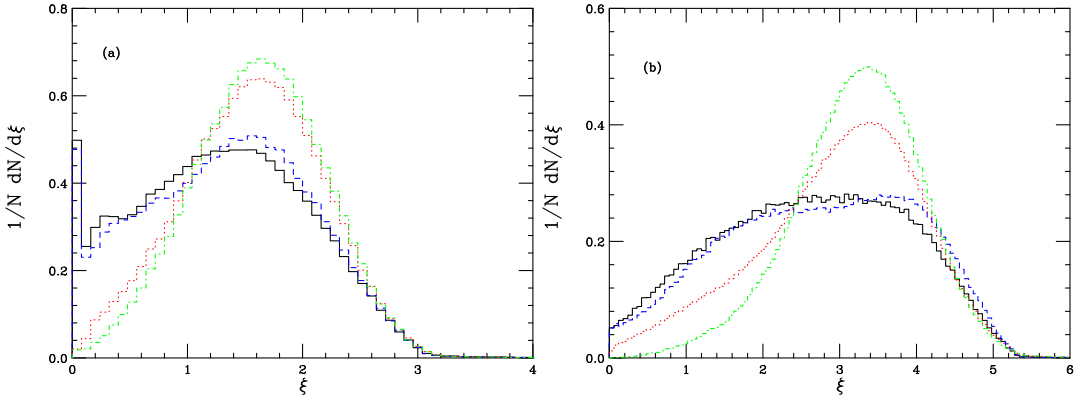

Figure 8. ξ spectrum for fixed and variable L. In the plots we follow the conventions adopted in figures 6 and 7.

JHEP11(2009)122

For the purpose of our phenomenological analysis, we included in HERWIG a fictitious process, where a shower is originated by a single gluon with energy 10 and 100 GeV. We studied the usual vacuum case, as well as showers in a medium characterized by transport coefficient $\hat{q}$ and length L, with L varying throughout the parton cascade. As HERWIG showers satisfy angular ordering, when starting with just one parton and not with a pair of colour-connected ones, we had to set by hand the upper value of the evolution variable.

We ran HERWIG with modified splitting functions and, first of all, observed that the average parton multiplicity in a medium is higher than in the vacuum, with an enhancement which varies from 20% to 80% when the accumulated transverse momentum $\hat{q}L_0$ runs between 2 and 50 GeV^2. Then, we studied differential distributions, such as transverse momentum (p_T), angle (θ) and logarithmic energy-fraction (ξ) spectra. Indeed, we found the features which one should expect in a dense medium with respect to the vacuum: enhancement at small p_T and suppression at high p_T, more partons at large angles, suppression at low ξ, compensating an enhancement for middle-high ξ values. As for the results obtained for $E = 10$ GeV, we noticed a sharp peak at $p_T = \theta = \xi = 0$, corresponding to a fraction of events with no emission at all. For this reason, we also plotted the ξ integrated distribution, which is insensitive to such a peak, and found results more similar to the ones yielded the Q-PYTHIA code and in qualitative agreement with the observations at RHIC. We investigated the differential spectra for fixed values of the length and found stronger medium effects, as in this case L does not decrease throughout the shower and is always positive.

As for the comparison with the results in [12], overall we found acceptable qualitative agreement, although, due to the fact that the two shower algorithms are pretty different and that we have been considering unphysical parton-level quantities, with hadronization switched off, some quantitative discrepancies are well visible. In fact, we observed that due to the choice of the showering variables, more branchings are simulated in PYTHIA, at least when using the default parametrizations, even before including medium modifications. In particular, sharp zero-peaks, exhibited by all HERWIG distributions when considering a starting gluon of 10 GeV, were not present in PYTHIA.

We believe that it will be now very interesting to consider an actual physical process, e.g. at the LHC, investigate hadron-level observables and eventually understand how, after including medium splitting functions, modified HERWIG fares with respect to Q-PYTHIA. For such a comparison to be trustworthy, both generators should be tuned to the same data set. Also, it will be very useful understanding whether the medium-induced effects found in this analysis still persist once hadronization is turned on. As for the issue of angular ordering and evolution variables, it will be cumbersome studying quantities sensitive to colour coherence or non-global observables, as in refs. [15, 17], and understand whether the discrepancies between HERWIG and PYTHIA still persist or medium-effect implementations wash them out. However, as we said in the introduction, a comparison with hadron-hadron and heavy-ion data is compulsory before making any strong statement on the role played by the shower evolution variable in a dense medium. The documentation of the Q-HERWIG code, including medium-modified splitting functions, which should be not seen as an official release, but rather as an add-up to the latest fortran version [5], is currently in progress [24].

JHEP11(2009)122

Acknowledgments

We acknowledge M.H. Seymour and U.A. Wiedemann for discussions on these and related topics. This work has been supported by Ministerio de Ciencia e Innovación of Spain under projects FPA2005-01963, FPA2008-01177 and contracts Ramón y Cajal (N.A. and C.A.S.), by Xunta de Galicia (Consellería de Educación and Consellería de Innovación e Industria — Programa Incite) (N.A. and C.A.S.), by the Spanish Consolider-Ingenio 2010 Programme CPAN (CSD2007-00042) (N.A. and C.A.S.), by the European Commission grant PERG02-GA-2007-224770 and Xunta de Galicia (Consellería de Educación e Ordenación Universitaria) (C.A.S.).

JHEP11(2009)122

References

[1] STAR collaboration, J. Adams et al., *Experimental and theoretical challenges in the search for the quark gluon plasma: the STAR collaboration's critical assessment of the evidence from RHIC collisions*, *Nucl. Phys.* **A 757** (2005) 102 [nucl-ex/0501009] [SPIRES];
B.B. Back et al., *The PHOBOS perspective on discoveries at RHIC*, *Nucl. Phys.* **A 757** (2005) 28 [nucl-ex/0410022] [SPIRES];
BRAHMS collaboration, I. Arsene et al., *Quark gluon plasma an color glass condensate at RHIC? The perspective from the BRAHMS experiment*, *Nucl. Phys.* **A 757** (2005) 1 [nucl-ex/0410020] [SPIRES];
PHENIX collaboration, K. Adcox et al., *Formation of dense partonic matter in relativistic nucleus nucleus collisions at RHIC: experimental evaluation by the PHENIX collaboration*, *Nucl. Phys.* **A 757** (2005) 184 [nucl-ex/0410003] [SPIRES].

[2] R. Baier, D. Schiff and B.G. Zakharov, *Energy loss in perturbative QCD*, *Ann. Rev. Nucl. Part. Sci.* **50** (2000) 37 [hep-ph/0002198] [SPIRES];
M. Gyulassy, I. Vitev, X.-N. Wang and B.-W. Zhang, *Jet quenching and radiative energy loss in dense nuclear matter*, nucl-th/0302077 [SPIRES];
A. Kovner and U.A. Wiedemann, *Gluon radiation and parton energy loss*, hep-ph/0304151 [SPIRES];
J. Casalderrey-Solana and C.A. Salgado, *Introductory lectures on jet quenching in heavy ion collisions*, *Acta Phys. Polon.* **B 38** (2007) 3731 [arXiv:0712.3443] [SPIRES];
D. d'Enterria, *Jet quenching*, arXiv:0902.2011 [SPIRES];
R. Baier, Y.L. Dokshitzer, A.H. Mueller, S. Peigne and D. Schiff, *Radiative energy loss and p_T-broadening of high energy partons in nuclei*, *Nucl. Phys.* **B 484** (1997) 265 [hep-ph/9608322] [SPIRES].

[3] R. Baier, Y.L. Dokshitzer, A.H. Mueller and D. Schiff, *Quenching of hadron spectra in media*, *JHEP* **09** (2001) 033 [hep-ph/0106347] [SPIRES].

[4] C.A. Salgado and U.A. Wiedemann, *Calculating quenching weights*, *Phys. Rev.* **D 68** (2003) 014008 [hep-ph/0302184] [SPIRES].

[5] G. Corcella et al., *HERWIG* 6.5*: an event generator for Hadron Emission Reactions With Interfering Gluons (including supersymmetric processes)*, *JHEP* **01** (2001) 010 [hep-ph/0011363] [SPIRES].

[6] V.A. Khoze, A.D. Martin and M.G. Ryskin, *On the role of hard rescattering in exclusive diffractive Higgs production*, *JHEP* **05** (2006) 036 [hep-ph/0602247] [SPIRES].

[7] ALICE collaboration, B. Alessandro, (ed.) et al., *ALICE: physics performance report, volume II*, *J. Phys.* **G 32** (2006) 1295 [SPIRES];
ALICE collaboration, F. Carminati, (ed.) et al., *ALICE: physics performance report, volume I*, *J. Phys.* **G 30** (2004) 1517 [SPIRES].

[8] CMS collaboration, D.G. d'Enterria, (Ed.) et al., *CMS physics technical design report: addendum on high density QCD with heavy ions*, *J. Phys.* **G 34** (2007) 2307 [SPIRES].

[9] ATLAS collaboration, P. Steinberg, *Heavy ion physics at the LHC with the ATLAS detector*, *J. Phys.* **G 34** (2007) S527 [arXiv:0705.0382] [SPIRES].

[10] A.D. Polosa and C.A. Salgado, *Jet shapes in opaque media*, *Phys. Rev.* **C 75** (2007) 041901 [hep-ph/0607295] [SPIRES].

[11] N. Armesto, L. Cunqueiro, C.A. Salgado and W.-C. Xiang, *Medium-evolved fragmentation functions*, *JHEP* **02** (2008) 048 [arXiv:0710.3073] [SPIRES].

[12] N. Armesto, L. Cunqueiro and C.A. Salgado, *Q-PYTHIA: a medium-modified implementation of final state radiation*, *Eur. Phys. J.* **C 63** (2009) 679 [arXiv:0907.1014] [SPIRES].

[13] See http://igfae.usc.es/qatmc/.

[14] G. Marchesini and B.R. Webber, *Simulation of QCD jets including soft gluon interference*, *Nucl. Phys.* **B 238** (1984) 1 [SPIRES]; *Monte Carlo simulation of general hard processes with coherent QCD radiation*, *Nucl. Phys.* **B 310** (1988) 461 [SPIRES].

[15] CDF collaboration, F. Abe et al., *Evidence for color coherence in $p\bar{p}$ collisions at $\sqrt{s} = 1.8$ TeV*, *Phys. Rev.* **D 50** (1994) 5562 [SPIRES].

[16] T. Sjöstrand and P.Z. Skands, *Transverse-momentum-ordered showers and interleaved multiple interactions*, *Eur. Phys. J.* **C 39** (2005) 129 [hep-ph/0408302] [SPIRES].

[17] A. Banfi, G. Corcella and M. Dasgupta, *Angular ordering and parton showers for non-global QCD observables*, *JHEP* **03** (2007) 050 [hep-ph/0612282] [SPIRES].

[18] M. Dasgupta and G.P. Salam, *Resummation of non-global QCD observables*, *Phys. Lett.* **B 512** (2001) 323 [hep-ph/0104277] [SPIRES].

[19] B.R. Webber, *A QCD model for jet fragmentation including soft gluon interference*, *Nucl. Phys.* **B 238** (1984) 492 [SPIRES].

[20] B. Andersson, G. Gustafson, G. Ingelman and T. Sjöstrand, *Parton fragmentation and string dynamics*, *Phys. Rept.* **97** (1983) 31 [SPIRES].

[21] G. Corcella and V. Drollinger, *Bottom-quark fragmentation: comparing results from tuned event generators and resummed calculations*, *Nucl. Phys.* **B 730** (2005) 82 [hep-ph/0508013] [SPIRES].

[22] L.D. Landau and I. Pomeranchuk, *Electron cascade process at very high-energies*, *Dokl. Akad. Nauk Ser. Fiz.* **92** (1953) 735 [SPIRES];
A.B. Migdal, *Bremsstrahlung and pair production in condensed media at high-energies*, *Phys. Rev.* **103** (1956) 1811 [SPIRES].

[23] I.P. Lokhtin and A.M. Snigirev, *A model of jet quenching in ultrarelativistic heavy ion collisions and high-p_T hadron spectra at RHIC*, *Eur. Phys. J.* **C 45** (2006) 211 [hep-ph/0506189] [SPIRES];

JHEP11(2009)122

K. Zapp, G. Ingelman, J. Rathsman, J. Stachel and U.A. Wiedemann, *A Monte Carlo model for 'jet quenching'*, *Eur. Phys. J.* **C 60** (2009) 617 [arXiv:0804.3568] [SPIRES];
T. Renk, *Parton shower evolution in a 3D hydrodynamical medium*, *Phys. Rev.* **C 78** (2008) 034908 [arXiv:0806.0305] [SPIRES];
K. Zapp, J. Stachel and U.A. Wiedemann, *A local Monte Carlo implementation of the non-abelian Landau-Pomerantschuk-Migdal effect*, *Phys. Rev. Lett.* **103** (2009) 152302 [arXiv:0812.3888] [SPIRES];
B. Schenke, C. Gale and S. Jeon, *MARTINI: an event generator for relativistic heavy-ion collisions*, arXiv:0909.2037 [SPIRES].

[24] G. Corcella, *Q-HERWIG: an angular-ordered parton shower generator for jet quenching*, work in progress.

[25] M. Bahr et al., *HERWIG++ 2.2 release note*, arXiv:0804.3053 [SPIRES].

[26] T. Sjöstrand, S. Mrenna and P. Skands, *A brief introduction to PYTHIA 8.1*, *Comput. Phys. Commun.* **178** (2008) 852.

[27] S. Catani, B.R. Webber and G. Marchesini, *QCD coherent branching and semiinclusive processes at large x*, *Nucl. Phys.* **B 349** (1991) 635 [SPIRES].

[28] M.H. Seymour, *Matrix element corrections to parton shower algorithms*, *Comp. Phys. Commun.* **90** (1995) 95 [hep-ph/9410414] [SPIRES].

[29] G. Miu and T. Sjöstrand, *W production in an improved parton shower approach*, *Phys. Lett.* **B 449** (1999) 313 [hep-ph/9812455] [SPIRES].

[30] R. Baier, Y.L. Dokshitzer, A.H. Mueller, S. Peigne and D. Schiff, *Radiative energy loss and p_T-broadening of high energy partons in nuclei*, *Nucl. Phys.* **B 484** (1997) 265 [hep-ph/9608322] [SPIRES].

[31] B.G. Zakharov, *Radiative energy loss of high energy quarks in finite-size nuclear matter and quark-gluon plasma*, *JETP Lett.* **65** (1997) 615 [hep-ph/9704255] [SPIRES].

[32] U.A. Wiedemann, *Gluon radiation off hard quarks in a nuclear environment: opacity expansion*, *Nucl. Phys.* **B 588** (2000) 303 [hep-ph/0005129] [SPIRES].

[33] G. Corcella and M.H. Seymour, *Initial state radiation in simulations of vector boson production at hadron colliders*, *Nucl. Phys.* **B 565** (2000) 227 [hep-ph/9908388] [SPIRES].

JHEP11(2009)122